American Journal of Pathology, Vol. 161, No. 5, November 2002

Technical Advance

Isolation of Living Neurons from Human Elderly Brains Using the Immunomagnetic Sorting DNA-Linker System

Yoshihiro Konishi,* Kristina Lindholm,* Li-Bang Yang,* Rena Li,*† and Yong Shen*‡

From the Haldeman Laboratory of Molecular and Cellular Neurobiology and the Roberts Center for Alzheimer's Research,† Sun Health Research Institute, Sun City; and the Molecular and Cellular Biology Program,‡ Arizona State University, Tempe, Arizona*

Isolation and culture of mature neurons from affected brain regions during diseased states provide a well-suited *in vitro* model system to study age-related neurodegeneration under dynamic conditions at cellular levels. We have developed a novel technique to isolate living neurons from rapidly autopsied human elderly brains, and have succeeded in keeping them alive *in vitro*. Specifically, the parietal cortex blocks were fractionated by density gradients and further enriched for neurons by an immunomagnetic sorting DNA-linker technique. The postmortem interval averaged 2.6 hours. After isolation and purification of neurons using this technology, the cells were maintained *in vitro* for 2 weeks. Our evaluation revealed that 80% of the isolated cells were neurons and they exhibited neurotransmitter phenotypes (glutamate and γ-aminobutyric acid) as well as glutamate receptors. Studies on cell viability and calcium influx suggest that these isolated living cortical neurons still retain their typical neuronal functions. Our present study demonstrates that neurons isolated from human elderly brain autopsies can survive *in vitro* and maintain their functional properties. Our study has opened an opportunity to apply such neurons to dynamic pharmacological studies of neurological disorders at the single-cell level. *(Am J Pathol 2002, 161:1567–1576)*

Isolation of aged neurons from elderly brain autopsy samples and their survival *in vitro* are clearly necessary, because we believe that the cells from the human species, an appropriate developmental or disease state, and the afflicted brain regions would provide a more suitable *in vitro* model system for studies of age-related neurodegeneration. However, little success has been made in human elderly brain tissues by using conventional approaches. Historically, isolation of neurons from human brain autopsies or aged rodent brains was pioneered by McKhann and colleagues,[1] Iqbal and Tellez-Nagel,[2] Farooq and colleagues,[3] and Brewer[4] although those *in vitro* cells were isolated either from frozen tissue or elderly rat brains. Thus, keeping human neurons from elderly brains alive *in vitro* was not attempted. We have developed a novel way to isolate and enrich neurons from rapidly autopsied human elderly brain samples, by using an immunomagnetic sorting technique following a conventional gradient isolation, and have succeeded in keeping these neurons alive *in vitro* and characterizing them in detail. Thus, this new approach has several advantages. First, this approach allows us to harvest neurons with an excellent purity that was previously limited by the single use of gradient isolation by which heterogeneous cell types were obtained. Second, it can be adapted to study molecular and cellular mechanisms of particular cell types for which phenotype-specific antigens are available. Third, it allows us to identify, study, and follow living neurons from human elderly healthy brains and diseased brains, such as Alzheimer's disease, at the single-cell level.

Supported in part by grants from the Alzheimer's Association, the Edward Johnson Foundation, and the Neuroscience Education and Research Foundation.

Accepted for publication July 22, 2002.

Present address of Y. K.: Division of Food Sciences, Mimasaka Women's College, Tsuyama, Okayama, 708-8511 Japan. Present address of L.-B. Y.: Earle Chiles Institute of Molecular Biology and Cancer Research, Oregon Health Sciences University, Portland, OR 97213.

Address reprint requests to Dr. Yong Shen, Haldeman Laboratory of Molecular and Cellular Neurobiology, Sun Health Research Institute, 10515 West Santa Fe Dr., Sun City, AZ 85351. E-mail: yong.shen@sunhealth.org.

Materials and Methods

Neuronal Isolation and Cultures

Brain tissue for culture was obtained from rapidly autopsied brains of geriatric patients ($n = 30$) enrolled in the Sun Health Research Institute brain bank. The average age of the patients was 78 years and the gender was well matched. The postmortem interval was 2.6 hours on the average. The parietal cortex blocks were cut into slices, digested with papain (Worthington, Lakewood, NJ) and overlaid onto a discontinuous density gradient of Optiprep (Nycomed, Olso, Norway) ranging from ~1.006, 1.006 to 1.030, 1.030 to 1.037, 1.037 to 1.045, 1.045 to 1.100, and 1.100~ g/ml (15 to 60%) (top-to-bottom), respectively. The lower one-third of phase 5 (phase 5c) (1.085 to 1.100 g/ml) contained the richest cells bearing the morphology consistent with neurons,[5] thus brain cells fractionated into phase 5c were processed for further purification of neurons, which was accomplished by incubating the cells with tetanus toxin C fragment (Boehringer, Indianapolis, IN) that binds to cell-surface gangliosides present in neurons.[6,7] The cells then reacted with an anti-TTC mouse IgG (Boehringer) were subsequently separated by addition of Dynabeads (Dynal, Oslo, Norway), which had been coated with recombinant streptavidin via DNA linker (Dynal) followed by conjugation with a biotinylated goat anti-mouse IgG (Jackson ImmunoResearch, West Grove, PA). After selecting the bound cells in a Dynal magnetic particle concentrator and removal of the beads with DNase I, the enriched neuronal preparations were cultured in Neurobasal A with B27 supplement with anti-oxidants (Life Technologies, Inc., Grand Island, NY), containing 5 ng/ml of basic fibroblast growth factor, 50 ng/ml of nerve growth factor, 10 ng/ml of brain-derived neurotrophic factor, 10 ng/ml of epidermal growth factor (Life Technologies, Inc.) and 100 nmol/L of retinoic acid (Sigma Chemical Co., St. Louis, MO). Moreover, no antibiotics, glutamate, or aspartate were included in our neuron culture because they are toxic to the neurons.

Classical Cytochemical Analysis

The phase 5c cells 2 weeks after plating (2w-phase 5c cells) were processed for the classical cytochemical stains, including Nissl (1% cresyl violet), Oil Red O, and pyronin Y/methyl green. Methods for these commonly used stains are given in detail elsewhere.[8–10] When pyronin Y is used in combination with methyl green, pyronin Y stains RNA red, whereas methyl green stains DNA green in bright field. Pyronin Y preferentially binds to double-stranded RNA by intercalation, resulting in enhancement of red fluorescence. DNA binding of pyronin Y is blocked by the nonfluorescent dye, methyl green.[10,11]

Immunocytochemistry

The following antibodies were used in this study: anti-neurofilament protein (NFP) SMI33 (1:2000, Sternberger, Lutherville, MD), anti-microtubule-associated protein-2 (1:400, Boehringer), anti-neuron-specific enolase (1:3000, Polysciences, Warrington, PA), anti-neuron-specific class III β-tubulin (βIII) (1:2000, Berkley, Richmond, CA), anti-calbindin (1:1000, Swant, Bellinzona, Switzerland), anti-neuron cell surface antigen (NeuSu) (1:500; Chemicon, Temecula, CA), anti-tetanus toxin C fragment (1:500, Boehringer), anti-neuronal nuclei (NeuN) (1:50, Chemicon), and anti-RNA-binding neuronal protein called Hu (1:1000; gift of Dr. H. Furneaux, Sloan Kettering Institute, New York, NY).[12–16] Moreover, antibodies to glial fibrillary acidic protein (GFAP) (1:100; DAKO, Carpinteria, CA), NG2 chondroitin sulfate proteoglycan[17] (1:1000, Chemicon), LN-3 (1:200, ICN, Costa Mesa, CA), von Willebrand factor (vWF) (1:50, DAKO), fibronectin (1:1000, Sigma), and galactocerebroside (GalC) (1:100, Boehringer) were used for nonneuronal identification. An antibody that detects central nervous system stem cells, anti-Musashi (1:1000; gift of Dr. H. Okano, Keio University, Japan)[18–25] was also used. Antibodies against neurotransmitter-synthesizing enzymes and neurotransmitter receptors used were anti-phosphate-activated glutaminase (PAG) (1:1000; gift of Dr. T. Kaneko, Kyoto University, Japan),[26–28] glutamate decarboxylase (GAD) (1:2000, Chemicon), choline acetyltransferase (ChAT) (1:1000, Chemicon), *N*-methy-D-aspartate receptor type 1 (NMDAR1) (1:1000; PharMingen, La Jolla, CA), and α-amino-3-hydroxy-5-methyl-4-isoxazole propionic acid (AMPA)-type glutamate receptor types 2 and 4 (GluR2/4) (1:1000, PharMingen).

The 2w-phase 5c cells were fixed with 4% paraformaldehyde followed by fixation with methanol and incubated with a primary antibody followed by a biotin-conjugated secondary antibody (Vector Laboratories, Inc., Burlingame, CA; Jackson ImmunoResearch). Vectastain Elite kits (Vector Laboratories, Inc.), 3,3′-diaminobenzidine (DAB), or Nova RED (Vector Laboratories, Inc.), and Cy3- or Oregon Green 514-strepatavidin (Molecular Probes, Eugene, OR) were used for immunoenzymatic and fluorescence detection. Sudan Black B (1%) in 70% ethanol was used to quench autofluorescence.[29] No nonspecific binding occurred when the antibodies that had been obtained from private individuals were preabsorbed to the respective recombinant antigens, which is consist with previous publications.[13–16,19–25,28] Deletion and replacement of primary antibodies with nonimmune sera were techniques used as controls throughout to certify the specific binding of commercially available antibodies. The optimal dilution ratio for each primary antibody was determined using adequate positive and negative control cells. Amplification of the immunolabeling using the Tyramide Signal Amplification kit (NEN, Boston, MA) was applied in parallel for detecting neurotransmitters and their receptors.

Western Blotting

Cells were lysed with 1% Triton X-100 and 0.1% sodium dodecyl sulfate. Then 20 μg of cell lysate protein was electrophoresed on a 10% polyacrylamide-sodium dodecyl sulfate gel, and transferred onto a polyvinylidene

difluoride membrane (Millipore, Bedford, MA). The membrane was blocked in 5% nonfat milk, reacted with the anti-βIII or GFAP antibody, and then with a horseradish peroxidase-conjugated secondary antibody (Boehringer).

Cell Viability Tests

Four different assays of cell viability were performed for the 2w-phase 5c cells. For the trypan blue exclusion test, cells were incubated for 5 minutes with 0.04% trypan blue (Sigma).[30,31] Methods for the other assays are given in detail elsewhere.[32–35] LIVE/DEAD Viability/Cytotoxicity kits (Molecular Probes) used a 30-minute incubation of the cells with 4 μmol/L of acetoxymethyl (AM) ester of calcein (calcein AM) and 6 μmol/L of ethidium homodimer (EthD-1). LIVE/DEAD Reduced Biohazard Viability/Cytotoxicity kits (Molecular Probes) used a 15-minute incubation of the cells with the mixture of SYTO 10 and DEAD Red recommended by the manufacture. The cells were cultured with addition of 0.5 mg/ml of tetrazolium salt such as 3-(4,5-dimethyl thiazol-2-yl)-2,5-diphenyl tetrazolium bromide (MTT) (Molecular Probes) at 37°C, with micrographs taken 2 and 4 hours after the addition.[35]

Calcium Imaging

The 2w-phase 5c cells were loaded with 10 μmol/L of fluo-3 AM (Molecular Probes) in low potassium buffer[36–38] (in mmol/L: NaCl, 137; $NaHCO_3$, 4.2; Na_2HPO_4, 0.34; KCl, 5.4; KH_2PO_4, 0.44; $MgSO_4$, 0.81; $CaCl_2$, 1.26; D-glucose, 5.55; HEPES, 20; pH 7.4) for 1 hour at 37°C in a CO_2 incubator, then processed for calcium optical recordings. Calcium influx was induced by exposing the cells to a 50 or 100 mmol/L of potassium buffer identical to the low potassium buffer, except that 92.4 or 42.4 mmol/L of NaCl and 50 or 100 mmol/L of KCl, respectively, were used. Calcium influx was also examined by using glutamate at concentrations ranging from 1 to 500 μmol/L. The fluo-3 fluorescence in the loaded cells was measured with Fluoview software (Olympus) and a confocal laser-scanning microscope system mounted to an inverted microscope (Olympus). Excitation was provided by the 488-nm line of an argon laser (NEC), and emission was collected at a wavelength >505 nm. Images were obtained every 2 seconds, and the significant changes in intracellular intensity were confirmed by recording background fluorescence intensity in parallel. Other buffers used were: calcium-free low potassium buffer[36–38] (in mmol/L: NaCl, 137; KCl, 5.4; $MgCl_2$, 2.07; EGTA, 5.0; D-glucose, 5.55; HEPES, 20; pH 7.4); manganese (or cobalt)-containing low potassium buffer[37,38] (in mmol/L: NaCl, 137; KCl, 5.4; $MgCl_2$, 2.07; $MnCl_2$, or $CoCl_2$, 4.0; D-glucose, 5.55; HEPES, 20; pH 7.4).

Results

Neuronal Characterizations

Our gradient isolation technique yielded six phases from the brain tissues. With phase microscopy, the lower one-third of phase 5 (phase 5c) most abundantly contained cells bearing the morphology consistent with neurons,[5] along with much debris (Figure 1a). The neuron-like cells accounted for 62.1 ± 3.6% ($n = 6$) of the phase 5c cellular components, when observed after 2 weeks *in vitro*. After further purification with the immunomagnetic sorting technique, in which magnetic beads coated with streptavidin via DNA linker were used (Figure 1, b and c), observation with phase microscopy after 2 weeks *in vitro* revealed that 86.9 ± 3.3% ($n = 6$) of the phase 5c cells were neuron-like cells (Figure 1d). The immunomagnetic purification from the phase 5c yielded approximately 1×10^6 cells/g tissue weight. These cells were multi-polar to mono-polar, fusiform, or triangular, and bore cell processes (Figure 1; e, f, and h). A relatively large nucleus and nucleolus were conspicuous (Figure 1g).

To characterize these neuron-like cells, classical cytochemical techniques were used: Nissl, Oil Red O, and pyronin Y stains. With Nissl staining, the nuclei were relatively unstained but the nucleoli were stained blue or purple (Figure 2, a and b). The granular materials that accumulated in the cytoplasm were usually stained blue or greenish-blue (Figure 2b). With Oil Red O or pyronin Y staining, these granules were stained red under bright-field viewing (Figure 2, c1 and d). With pyronin Y combined with methyl green, these granules produced a relatively low red fluorescence (Figure 2,c2), suggesting that these granules are lipofuscin, which has been reported to include lipids,[39] but not Nissl bodies. Nissl staining evaluations suggested that 81.5 ± 6.1% ($n = 6$) of the 2w-phase 5c cells were neurons.

To further ensure that these cells were neurons, we characterized them with immunocytochemistry. For neuron-specific cytoplasmic markers, antibodies against NFP (SMI33), microtubule-associated protein-2, neuron-specific enolase, βIII, and calbindin were used. The representative staining for NFP(SWI33) or βIII is shown in Figure 3A, a and b series. For a neuron-specific cell surface marker, antibody for NeuSu was used (Figure 3A, c). Lastly, we used antibodies against neuron-specific nuclear protein, NeuN and Hu[12] on these neurons. Figure 3A, d2, demonstrates a representative immunofluorescent staining of NeuN. The fluorescent staining shown was not quenched by using Sudan Black B[29] for exclusion of overlapping by autofluorescence. Thus, the immunofluorescence observed with the neuron staining is specific. Quantitative evaluations on the 2w-phase 5c cells revealed that 60 to 80% ($n = 10$) of the total cells were immunoreactive to these neuronal markers (Table 1). Meanwhile, quantitative analysis of percentages of cells showing immunoreactivity for nonneuronal antigens such as GFAP, LN-3, vWF, NG2[17] in the total cell population (Figure 3B, a to d) from the 2w-phase 5c cells in Table 1 is consistent with the above findings whereas positive control cells, including astrocytes, microglial cells, endothelial cells, and progenitor cells show strong immunoreactive response, respectively (Figure 3B; e to h). We found that our phase 5c neurons lacked immunoreactivity for the neural RNA-binding protein Musashi[18] (Figure 3B, d), excluding the possibility that the neurons isolated were differentiated from *in vitro* replication of

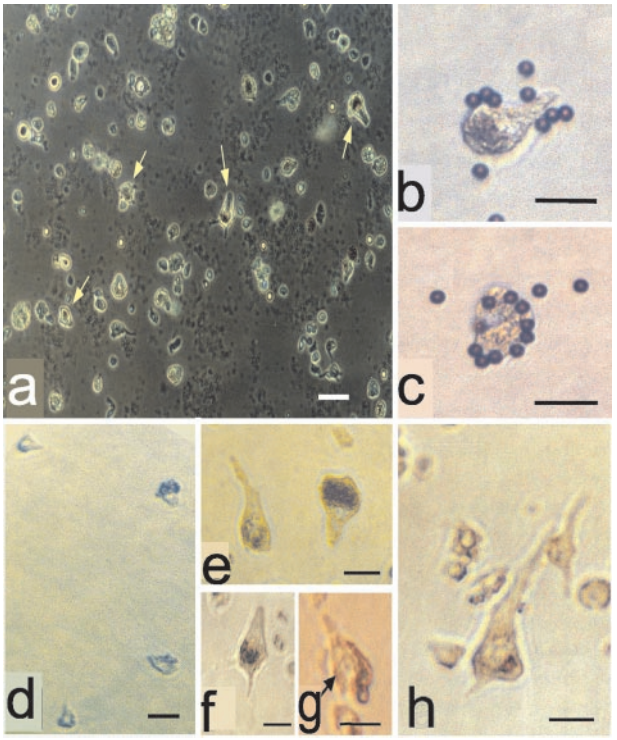

Figure 1. Immunomagnetic sorting and phase microscopic morphology. **a:** Cells from phase 5c after the gradient isolation were maintained *in vitro* for 2 weeks. This population contained much cell debris. **Arrows** indicate the cells showing a bright cytoplasm. **b** and **c:** The cells were further purified by the immunomagnetic sorting technique. Magnetic beads coated with streptavidin via DNA linker were used. The phase 5c cells were incubated with tetanus toxin C fragment (TTC) followed by exposure to a mouse anti-TTC IgG, to which then the magnetic beads complexed with an anti-mouse IgG were reacted. The beads shown readily attached to the cells. **d:** The purified cells using the magnetic beads were maintained *in vitro* for 2 weeks. A relatively pure neuronal-cell population is observed. **e**, **f**, and **h:** Neuron-like cells obtained through the above-mentioned procedures were maintained *in vitro* for 2 weeks. The vast majority of such phase 5c cells exhibit the morphological characteristics of neurons. Brown lipofuscin granules, a typical hallmark for aged neurons, are seen. **g:** In such a neuron-like cell, the nucleus and nucleolus are conspicuous (**arrow**). Scale bars: 100 μm (**a**); 50 μm (**b**, **c**, **e**, **f**, **g**, and **h**); 75 μm (**d**).

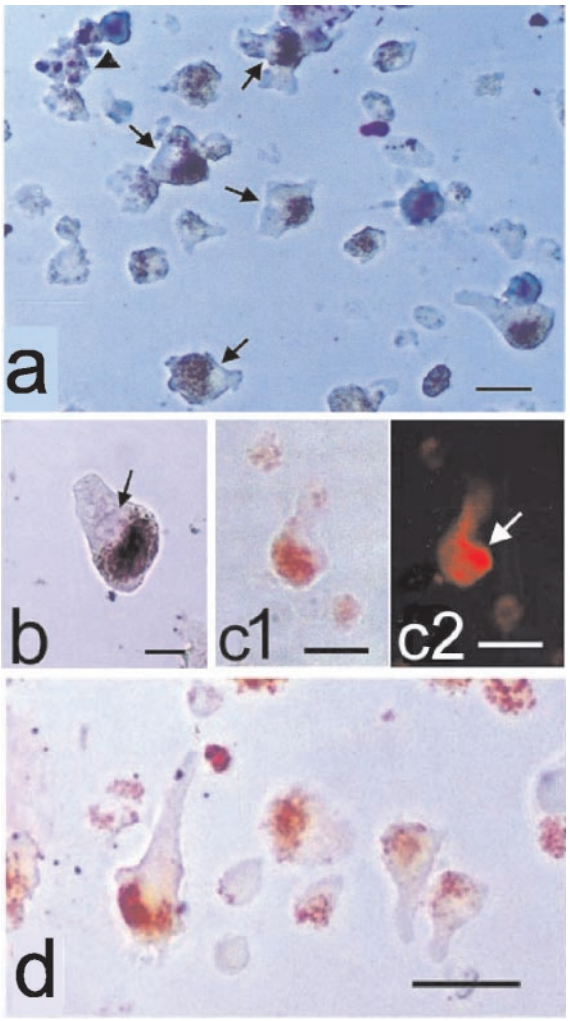

Figure 2. Classical cytochemistry. The phase 5c cells isolated through the immunomagnetic sorting were maintained for 2 weeks *in vitro*. **a:** Nissl-1. The nuclei of the phase 5c neuron-like cells are weakly stained at best (**arrows**). Lipofuscin granules are intensely stained blue or purple. An **arrowhead** indicates nonneuronal cells. **b:** Nissl-2. The lipofuscin granules are stained greenish-blue, a somewhat different color, compared to true Nissl bodies. The light blue staining is observed around the nucleus and in the nucleolus (**arrow**). **c:** Pyronin Y/methyl green. Under bright-field optics (**c1**), the lipofuscin granules are stained red. Under fluorescence optics (**c2**), however, these granules show relatively low red fluorescence, and by contrast the cytoplasm exhibit intense red fluorescence (**white arrow**). **d:** Oil Red O. The lipofuscin granules are labeled red. Scale bars: 50 μm (**a**, **c1**, **c2**); 25 μm (**b**); 100 μm (**d**).

stem cells. Western blot analysis further demonstrated that a single immunoreactive band for the neuron marker, β III at 50 kd was identified from our phase 5c neuron samples from autopsies of human elderly patients whereas this band was not observed for microglia or astrocyte samples, which were prepared in our facility[40] (Figure 3C). By contrast, an immunoreactive band for the astrocyte marker GFAP at the appropriate molecular weight of 50 kd was observed in the astrocyte samples but not in the microglia or phase 5c cells (Figure 3C).

Neurotransmitter Phenotypes

To examine what types of neurotransmitters these neurons contain, the neurons were evaluated for synthesizing enzymes for two typical cortical neurotransmitters, glutamate and γ-aminobutyric acid (GABA). We found that the antibody against the glutamate-synthesizing enzyme PAG[27] was immunoreactive to presumed glutamatergic neurons after the autofluorescence was quenched by Sudan Black B (Figure 4A, a2). Meanwhile, PAG-transfected cells were used as a positive control (Figure 4A, a3). Thus, we believe that the immunofluorescent staining was specific. By using the similar approach, we found that the antibody against GAD (67 kd) immunoreactively labeled presumed GABAergic neurons[41] (Figure 4A, b2). Lastly, we used an antibody to the acetylcholine-synthesizing enzyme ChAT to label presumed cholinergic neurons[42] and found little immunoreactive staining on these neurons (Figure 4A, c2). To quantitatively examine proportions of these neurons we isolated, we counted each type of neurotransmitter immunoreactive neurons. We found that PAG-positive neurons comprised 55.3 $\pm$ 18.5% (n = 6) of the 2w-phase 5c neuronal population, a low percentage compared to the estimated 70 to 80% prevalence of glutamatergic cells in the intact neocor-

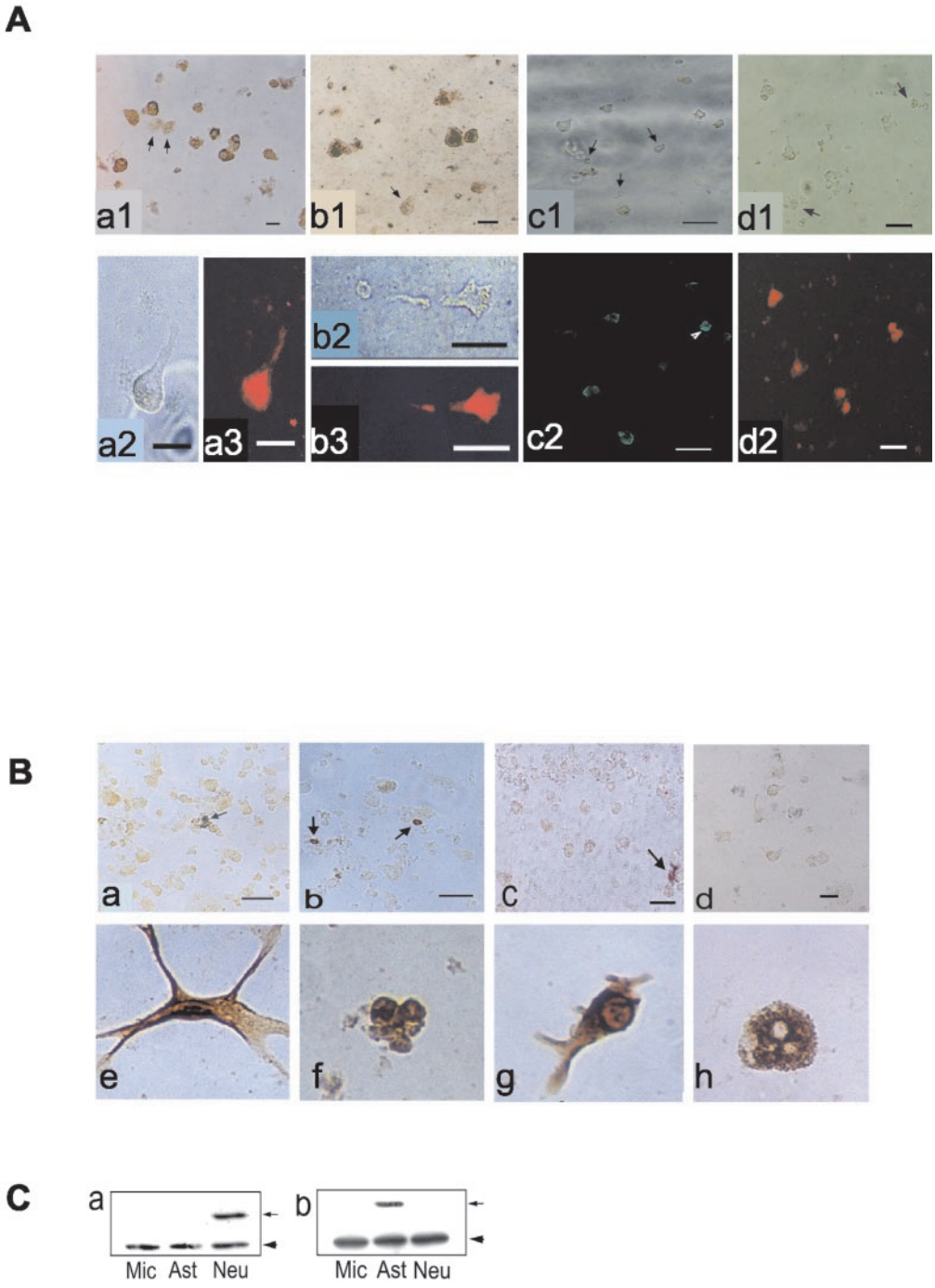

Figure 3. Immunocytochemistry of neuronal and nonneuronal markers. **A:** The phase 5c cells after 2 weeks *in vitro* were characterized for neuron-specific markers. Most of the phase 5c cells were consistently labeled with antibodies directed against the neuronal antigens. Neuron-specific cytoplasmic markers used were: neurofilament protein (NFP, SMI33) and neuron-specific class III β-tubulin (βIII). NFP was immunoreactive to the neurons, shown with DAB staining (**a1**) and also with Cy3 immunofluorescence (**a3**), **a2** is phase contrast of **a3**. **Arrows** in **a1** indicate unstained cells. Similarly, the neurons also show βIII-immunoreactive staining using DAB (**b1**) and Cy3 immunofluorescent methods (**b3**). **b2** is phase contrast of **b3**. Neuron-specific cell surface marker is NeuSu. **c1** is the same field visualized with phase contrast and **c2** is NeuSu immunofluorescence using Oregon Green marker. **Arrows** in **c1** indicate unstained cells and a **white arrowhead** in **c2** indicates lipofuscin-derived cytoplasmic autofluorescence. Neuron-specific nuclear marker, neuronal nuclei (NeuN) shows labeled neuronal nuclei. **d1** is the same field visualized with phase contrast and **d2** is NeuN immunofluorescence using Oregon Red marker. **Arrows** in **d1** also indicate unstained cells. **B:** The phase 5c cells after 2 weeks *in vitro* were characterized for nonneuronal markers. Less than 10% of the total phase 5c cell population was immunoreactive to nonneuronal markers tested. The neurons show negative DAB immunoreactivity to antibodies of GFAP (**a**), LN-3 (**b**), von Willebrand factor (vWF) (**c**), and Musashi (**d**) with a DAB marker. **Arrows** in **a** to **c** indicate occasionally stained cells. In parallel, each positive control cell type is demonstrated: primary astrocyte (**e**),[40] primary microglia (**f**),[40] isolated capillary (**g**), and NG108 neuroblastoma cell (**h**). **C:** Western blot analysis for the neuronal marker βIII (**a**) and the astrocytic marker GFAP (**b**) was performed using protein extracts obtained from primary microglia (Mic) and astrocyte (Ast) cultures, and isolated phase 5c cells (Neu) 2 weeks after plating from rapid autopsies of human elderly brains. **Arrows** indicate specific immunoreactive bands for βIII (**a**) and GFAP (**b**). **Arrowheads** illustrate bands for β-actin. Scale bars: [50 μm (**A:**a1, **a2**, **a3**, **b1**, **b2**, **b3**; **B d**, **f**, **g**, and **h**); 100 μm (**A:**c1, **c2**, **d1**, **d2**; **B: a**, **b**, **c**, and **e**).

Table 1A. Percentages* of the Phase 5c Cells Labeled with Neuron-Specific Markers

Markers (cytoplasmic)	Positive cells (%)	Markers (cell surface)	Positive cells (%)	Markers (nucleus)	Positive cells (%)
NFP	78.8 ± 5.9†	NeuSu	63.2 ± 8.1	NeuN	69.3 ± 12.3
MAP-2	68.9 ± 1.0	TTC	86.8 ± 9.0	Hu	80.6 ± 12.1
NSE	94.0 ± 7.8				
βIII	69.4 ± 1.1				
Calbindin	51.8 ± 3.1				

NFP, neurofilament protein (SMI33); MAP-2, microtubule-associated protein-2; NSE, neuron specific enolase; βIII, neuron-specific class III β-tubulin; NeuSu, neuron cell surface antigen; TTC, tetanus toxin C fragment; NeuN, neuronal nuclei.
*Each percentage value was calculated by using 10 of × 400 photomicrograms obtained from each of 10 autopsy cases.
†Mean ± SD.

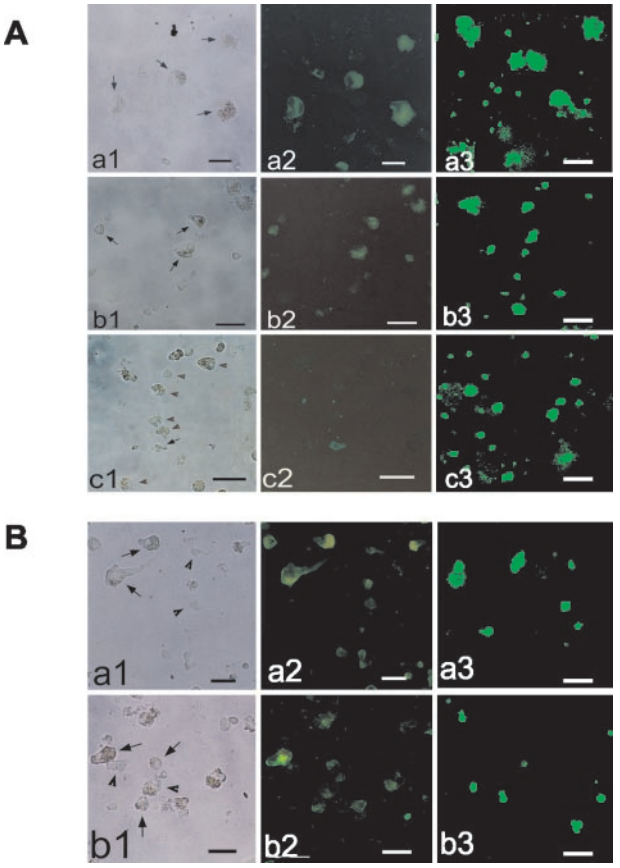

Figure 4. Neurotransmitter and receptor phenotypes. **A:** The phase 5c cells after 2 weeks *in vitro* were evaluated for phenotypes of neurotransmitters by immunocytochemistry enhanced with the tyramide signal amplification technique. **a:** PAG for glutamatergic neurons; **b:** GAD for GABAergic neurons; and **c:** ChAT for cholinergic neurons. The first (**a1**, **b1**, and **c1**) and second (**a2**, **b2**, and **c2**) columns in each series are the same field visualized with phase contrast and fluorescence using Oregon Green marker, respectively. Specific fluorescence in the cytoplasm was observed after lipofuscin autofluorescence was quenched by a Sudan Black B treatment. **Arrows** and **arrowheads** in the first column indicate significantly stained and unstained cells, respectively. The third column demonstrates specific immunofluorescent staining in each corresponding transfected cells as positive controls: **a3**, transiently transfected PAG HEK293 cells; **b3**, transiently transfected GAD HEK293 cells; **c3**, transiently transfected ChAT HEK293 cells. **B**: **a**, NMDA receptor type 1 (NMDAR-1); **b**, AMPA-type glutamate receptor types 2/4 (GluR^{2}4). The first (**a1** and **b1**) and second (**a2** and **b2**) columns in each series are the same field visualized with phase contrast and fluorescence using Oregon Green marker, respectively. Specific fluorescence in the cytoplasmic membrane was obtained after lipofuscin autofluorescence was quenched by a Sudan Black B treatment. **Arrows** and **arrowheads** in **a1** and **b1** indicate significantly stained and unstained cells, respectively. The third column pictures are transiently transfected NMDR1 HEK293 cells (**a3**) and transiently transfected GluR^{2}4 HEK293 cells (**b3**) as positive controls. Scale bars: 50 μm (**A:**a1 to **a3**; **B: a1** to **d3, b1** to **b3**); 100 μm (**A:**b1 to **b3, c1** to **c3**).

tex[43] (Table 2). GAD-immunoreactive cells comprised 52.3 ± 12.3% (n = 6) of the 2w-phase 5c neuronal population, a percentage somewhat higher than that observed in the human cortex *in situ*[44,45] (Table 2). These results are consistent with a relative resistance of GABAergic neurons to ischemia and a heightened sensitivity of glutamatergic neurons to ischemia, as previously reported.[46–48] Immunoreactivity for ChAT was evident in only 9.5 ± 1.9% (n = 6) of the 2w-phase 5c neuronal population. A similarly low percentage of ChAT-positive neurons have been observed in sections from the human adult neocortex[49] (Table 2). Many neurons in the cerebral cortex receive glutamatergic input.[50] We

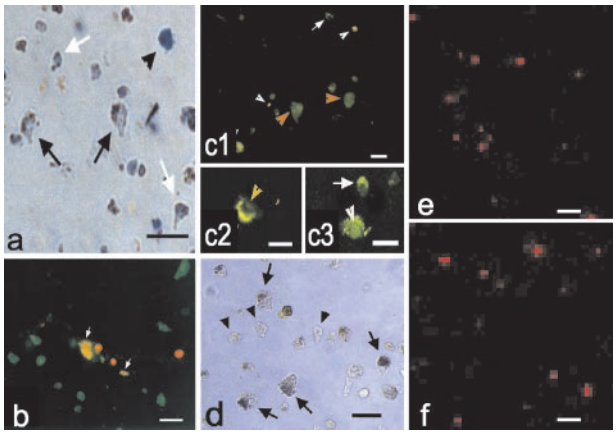

Figure 5. Biochemical evaluation of cell viability. The phase 5c cells after 2 weeks *in vitro* were assayed for their viability. **a:** Trypan blue (0.04%). Trypan blue incorporation into our neurons ranges from a clear cytoplasm (**black arrows**) to a pale blue cytoplasm (**white arrows**), with occasionally intense blue staining (**arrowhead**). Cell viability was further confirmed by the following rigorous cell viability: **b**: Calcein AM/ethidium homodimer (EthD-1) staining. Green cytoplasmic fluorescence and red nuclear fluorescence are observed. **Arrows** indicate yellowish autofluorescence that are easily identified because of distinct wavelengths. **c:** SYTO 10/DEAD Red staining. **White arrows** and **white arrowheads** (**c1**) indicate unlabeled cells with both dyes and red-labeled nuclei with indication of being dead, respectively. **Orange arrowheads** indicate viable cells (stained with SYTO10 in the presence of DEAD Red). Differences are observed between the nuclear labeling when the cells were incubated for 15 minutes (**c2**) and 1 hour (**c3**). A **yellow arrowhead** in **c2** indicates a labeled nucleus, and an **arrow** and an **arrowhead** in **c3** indicates an unlabeled cell and a labeled nucleus, respectively. Meanwhile, dead neurons isolated from frozen tissues stained with Calcein AM/EthD-1 and SYTO 10/DEAD Red are demonstrated in **e** and **f**, serving as control groups. To further rule out a possibility of autofluorescence, the tetrazolium salt MTT was used on these neurons. **d:** The exposure of MTT to living neurons produces purple formazans. Dark blue formazans are shown within living cells as a granular duster in approximately 80% of the neurons (**arrows**), whereas no formazans are formed in nonstained cells (**arrowheads**), indicating cell death. Scale bars: 100 μm (**a**, **b**, **c1**, **e**, **f**); 75 μm (**d**); 50 μm (**c2**, **c3**).

Table 1B. Percentages* of the Phase 5c Cells Labeled with Nonneuron-Specific Markers

Markers	Positive cells (%)	Cells detected
GFAP	9.4 ± 7.3†	Astrocytes
LN-3	8.9 ± 2.5	Microglia/macrophages
vWF	9.5 ± 7.8	Endothelial cells
NG2	3.7 ± 3.6	O-2A progenitors, type 2 astrocytes
Fibronectin	6.8 ± 1.0	Fibroblasts

GFAP, glial fibrillary acidic protein; vWF, von Willebrand factor; O-2A, oligodendrocyte-type 2 astrocyte.
*Each percentage value was calculated by using 10 of ×400 photomicrograms obtained from each of 10 autopsy cases.
†Mean ± SD.

examined whether our neurons expressed glutamate-related receptors by using antibodies directed against NMDAR1 and GluR2/4. Immunoreactivity for the NMDAR1 and GluR2/4 was present in 74.2 ± 10.2% and 77.1 ± 6.4% ($n = 6$) of the 2w-phase 5c neurons, respectively. This immunoreactivity was typically localized to the cell membrane, a result more clearly visualized after Sudan Black B treatment to reduce lipofuscin autofluorescence[29] (Figure 4B, a2 and b2).

Biochemical Evaluation of Neuronal Viability

To evaluate whether these neurons were alive, four different assays of cell viability were performed after 2 weeks *in vitro*. With the trypan blue exclusion test, the 2w-phase 5c cells with neuronal morphology ranged from having a clear cytoplasm to having a pale blue cytoplasm, with only occasionally an intense blue staining (Figure 5a). Trypan blue can passively be taken by injured cells through their permeable membrane or even enter viable cells with some injury by trypsinization.[30,31] Thus, these isolated neurons were further examined by using more rigorous cell viability techniques. With calcein AM plus EthD-1 (Figure 5b), 80.8 ± 10.5% ($n = 10$) of the 2w-phase 5c neurons significantly showed green cytoplasmic fluorescence, indicative of viability,[32,33] and 6.7 ± 1.6% ($n = 10$) exhibited red nuclear fluorescence, indicating cell death[32,33] (Table 3). To further confirm these findings, we conducted this assay for isolated dead neurons from frozen tissue of the same brain region. We found that all cells demonstrated red nuclear fluorescence (Figure 5e).

Next, we used the mixture of SYTO 10 and DEAD Red, by which living cells appear fluorescent green and dead cells appear fluorescent red.[32,33] After a 15-minute incubation, 69.9 ± 9.2% ($n = 6$) of the neurons exhibited fluorescent green nuclei, and 8.3 ± 7.3% ($n = 6$) showed red nuclear fluorescence (Figure 5c1). When the incubation time was 1 hour, 82.1 ± 5.9% ($n = 6$) fluoresced green and 10.1 ± 8.3% ($n = 6$) exhibited red or yellowish orange fluorescent nuclei (Figure 5, c2 and c3) (Table 3). Such a yellowish signal may mean that both SYTO 10 and DEAD Red have bound nucleic acids.[34] To further verify these results, the dead neurons isolated from the frozen tissue of the same brain region were used as control cells, showing that all of the dead neurons exhibited red nuclei (Figure 5f).

Table 2. Neurotransmitter Phenotypes of Neurons in the Phase 5c

Markers	Neurotransmitters	Positive cells (%)*	Percentage in the intact cortex‡ (%)
PAG	Glutamate	55.3 ± 18.5†	70–80
GAD	GABA	53.2 ± 12.3	30–40
ChAT	ACh	9.5 ± 1.9	~10

PAG, phosphate-activated glutaminase; GAD, glutamate decarboxylase; ChAT, choline acetyltransferase; ACh, acetylcholine.
*Each percentage value was calculated by using 10 of ×400 photomicrograms obtained from each of 6 autopsy cases.
†Mean ± SD.
‡Reported by immunohistochemistry in humans or primates.

Lastly, besides using Sudan Black B to avoid any possibility of lipofusin autofluorescence, we also used tetrazolium salts such as MTT, which are evaluated in bright field but not by fluorescence. Specifically, we examined mitochondrial function with six different formazans.[51] Tetrazolium salts, including MTT, form purple or orange formazans after exposure to the tetrazolium salts in living but not dead cells. After incubation of the 2w-phase 5c cells with MTT (Figure 5d), fine granular purple formazans were recognized in 77.0 ± 8.7% ($n = 6$) of the 2w-phase 5c neuron-like cells (Table 3). The formazans exhibited a granular appearance, as in a previous report.[35]

Calcium Imaging Studies

To examine whether these neurons retain a typical neuronal function, calcium influx in the neurons was monitored using the calcium-imaging technique. When neurons from individuals (<60 years old) were depolarized by applying 50 to 100 mmol/L of potassium chloride (high KCl), we found that 78.3 ± 14.4% ($n = 6$) of the neurons exhibited the expected rapid increase in intracellular fluo-3-derived fluorescence intensity 2 to 5 seconds after the high KCl application (Figure 6a). The KCl-induced fluorescence increments were quenched if calcium in the buffer was subsequently replaced with manganese (Figure 6b) or cobalt (not shown), and no increments occurred if calcium-free buffer was used initially (Figure 6c). On the other hand, the percentage of neurons exhibiting KCl-induced fluorescence increases was lower (42.5 ±

Table 3. Percentages* of the Living and Dead Neurons Estimated by Different Cell Viability Tests

Live markers	Living cells (%)	Dead markers	Dead cells (%)
Calcein AM	80.8 ± 10.5†	Ethidium homodimer	6.7 ± 1.6
SYTO 10	82.1 ± 5.9	DEAD Red	10.1 ± 8.3
MTT	77.0 ± 8.7		

MTT, 3-(4,5-dimethyl thiazol-2-yl)-2,5-diphenyl tetrazolium bromide.
*Each percentage value was calculated by using 10 of ×400 photomicrograms obtained from each of 6 or 10 autopsy cases.
†Mean ± SD.

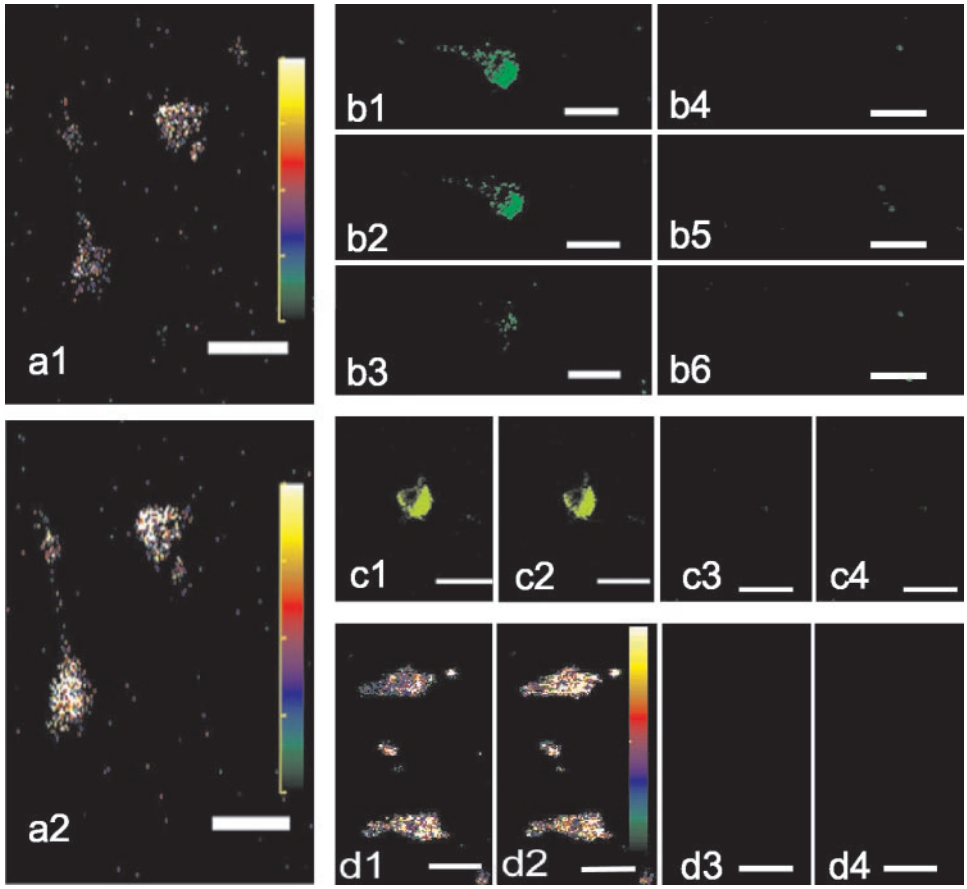

Figure 6. Calcium influx in human aged cortical neurons. The phase 5c cells after 2 weeks *in vitro* were loaded with fluo-3 AM and depolarized by 50- to 100-mmol/L KCl (high KCl) or 100- to 500-μmol/L glutamate. **a:** Pseudocolor-enhanced photomicrograms. Pictures are the same field before (**a1**) and 2 seconds after (**a2**) high KCl application. In the color scale bars, upper colors show higher fluorescence intensity. High KCl-induced fluorescence increments are quenched when calcium in the buffer is subsequently replaced with manganese (**b1**, before; **b2**, 5 seconds after; **b3**, 10 seconds after replacement). The same treatments of high KCl and replacement of manganese were applied on dead neurons isolated from frozen tissue of the same brain region and no calcium influx was observed (**b4** to **b6**). Furthermore, neurons exhibit no high KCl-induced increase in intracellular fluorescence intensity when calcium is initially removed (**c1**, before; **c2**, 10 seconds after high KCl application) whereas no calcium influx was observed with the same treatment in the dead neurons isolated from frozen brain tissue (**c3** and **c4**). **b1** to **b6** and **c1** to **c4** were obtained at the different voltages for the 488-nm line of an argon laser. Furthermore, 500 μmol/L of glutamate induces calcium influx (**d1**, before; **d2**, 10 seconds after the treatments) whereas no calcium influx was observed with the same treatment in the dead neurons isolated from frozen brain tissue (**d3** and **d4**). Scale bars, 75 μm.

25.6%, $n = 6$) if the neurons were isolated from relatively older (>70 years old) individuals. Furthermore, as expected in that more than 70% of our 2w-phase 5c neurons express glutamate (NMDA and AMPA) receptors, an increased calcium influx was observed when they were loaded with fluo-3 AM followed by treatment with 100 to 500 μmol/L of glutamate (Figure 6d). They exhibited the expected rapid increase in intracellular fluo-3-derived fluorescent intensity 5 to 10 seconds after the glutamate treatment. The result suggests that glutamate can induce a typical neuronal increase of calcium influx. From the above experiments on calcium influx, no calcium influx was observed in the dead neurons isolated from frozen brain tissue (Figure 6, b4 to b6, c3 to c4, d3 to d4).

Discussion

To our knowledge, this is the first report of a new strategy for the identification, isolation, and enrichment of primary neurons obtained from rapidly autopsied human elderly brains using the immunomagnetic sorting technique bonded with the neuronal TTC. By providing an approach to identifying neurons while they are alive, even if they are aged, the use of immunomagnetic sorting technology with cell surface-specific markers such as TTC will allow the specification of phenotype to be studied on a single-cell level in real time. Furthermore, when used in conjunction with other antigens, this strategy might permit the enrichment of any neurotransmitter phenotypes or cell types with the phenotype-specific markers.

Besides our novel technique providing a unique opportunity, several other factors also contributed to this successful study. First, we believe that a short postmortem period (<3 hours) is extremely important for neuronal survival for the reason that a low yield or failure of neuronal survival has been obtained from autopsies with postmortem periods >6 hours. We also believe that our optimal combination of neurotrophic factors and antioxidants has played a critical role in the survival of these aged neurons.

Neurons with external applications of 50 to 100 mmol/L of KCl or 100 to 500 μmol/L of glutamate increased Ca^{2+}

influx. Because ion concentrations in the bathing buffer for our neurons were adjusted by decreasing sodium ion concentration as the KCl concentration was increased, thus, these neurons still existed under the same osmolarity of the bathing solution, and behaviors of these neurons in this culture are not expected to be different.[36–38] Moreover, it is possible that some of these isolated neurons may be degenerating neurons that have weak calcium signaling because they are from aged or diseased brains.[52,53] Even if unusual Ca^{2+} events may be involved, our report is the first to demonstrate KCl or glutamate-induced calcium influx in human aged neurons, indicating the possibility of further pharmacological studies.

Lastly, it should be emphasized that we understand that the neurons are not perfectly healthy and that they are isolated from autopsied brains of aged or sick patients. It is quite labor intensive to isolate and maintain aged or sick neurons *in vitro*. Nevertheless, RNA and neuronal proteins from our isolated living neurons are preserved, and enzymes and membranes are still functional, indicating that our study has provided the future possibility to apply such human aged neurons to dynamic pharmacological studies for age-related neurological disorders at the single-cell level.

Acknowledgments

We thank Dr. Thomas Beach for neuropathological examination; Ms. Lucia Sue, Ms. Sarah Scott, and Ms. Kathryn Layne for technical assistance to obtain rapidly autopsied brain tissues; Dr. Steven A. Goldman from the Cornell Medical School for helpful discussion at the early stage of this study; and Dr. Donald Price, The Johns Hopkins University, and Dr. Dennis Selkoe, Dr. Rudolph Tanzi, and Dr. Anne Young, Harvard Medical School, for their continuous encouragement and appreciation.

References

1. McKhann GM, Ho W, Raiborn C, Varon S: The isolation of neurons from normal and abnormal human cerebral cortex. Arch Neurol 1969, 20:542–547
2. Iqbal K, Tellez-Nagel I: Isolation of neurons and glial cells from normal and pathological human brains. Brain Res 1972, 45:296–301
3. Farooq M, Ferszt R, Moore CL, Norton WT: The isolation of cerebral neurons with partial retention of processes. Brain Res 1977, 124: 69–81
4. Brewer GJ: Isolation and culture of adult rat hippocampal neurons. J Neurosci Methods 1997, 71:143–155
5. Steward O: Cell biology of neurons. Principle of Cellular, Molecular, and Developmental Neuroscience. New York, Springer-Verlag, 1989, pp 1–41
6. Dimpfel W, Huang RT, Habermann E: Gangliosides in nervous tissue cultures and binding of ^{125}I-labeled tetanus toxin, a neuronal marker. J Neurochem 1977, 29:329–334
7. Williamson LC, Bateman KE, Clifford JCM, Neale EA: Neuronal sensitivity to tetanus toxin requires gangliosides. J Biol Chem 1999, 274:25173–25180
8. Sheehan DC, Hrapchak BB: Nuclear and cytoplasmic stains. Theory and Practice of Histopathology, ed 2. Colombia, Battelle Press, 1987, pp 137–158
9. Carson FL: Nerve tissue. Theory and Practice of Histopathology, ed 2. Edited by DC Sheehan, BB Hrapchak. Colombia, Battelle Press, 1987, pp 252–266
10. Darzynkiewicz Z: Simultaneous analysis of cellular RNA and DNA content. Methods Cell Biol 1994, 41:401–420
11. Green FJ (Ed) Pyronin Y. The Sigma-Aldrich Handbook of Stains, Dyes and Indicators. Milwaukee, Aldrich Chemical, 1990, pp 601–602
12. Szabo A, Dalmau J, Manley G, Rosenfeld M, Wong E, Henson J, Posner JB, Furneaux HM: HuD, a paraneoplastic encephalomyelitis antigen, contains RNA-binding domains and is homologous to Elav and Sex-lethal. Cell 1991, 67:325–333
13. Rauer S, Andreou I: Tumor progression and serum anti-HuD antibody concentration in patients with paraneoplastic neurological syndromes. Eur Neurol 2002, 47:189–195
14. Camdessanche JP, Antoine JC, Honnorat J, Vial C, Petiot P, Convers P, Michel D: Paraneoplastic peripheral neuropathy associated with anti-Hu antibodies: a clinical and electrophysiological study of 20 patients. Brain 2002, 125:166–175
15. Darnell RB, Furneaux HM, Posner JB: Antiserum from a patient with cerebellar degeneration identifies a novel protein in Purkinje cells, cortical neurons, and neuroectodermal tumors. J Neurosci 1991, 11:1224–1230
16. Fathallah-Shaykh H, Wolf S, Wong E, Posner JB, Furneaux HM: Cloning of a leucine-zipper protein recognized by the sera of patients with antibody-associated paraneoplastic cerebellar degeneration. Proc Natl Acad Sci USA 1991, 88:3451–3454
17. Stallcup WB, Beasley L: Bipotential glial precursor cells of the optic nerve express the NG2 proteoglycan. J Neurosci 1987, 7:2737–2744
18. Sakakibara S, Imai T, Hamaguchi K, Okabe M, Aruga J, Nakajima K, Yasutomi D, Nagata T, Kurihara Y, Uesugi S, Miyata T, Ogawa M, Mikoshiba K, Okano H: Mouse-Musashi-1, a neural RNA-binding protein highly enriched in the mammalian CNS stem cell. Dev Biol 1996, 176:230–242
19. Kaneko Y, Sakaibara S, Imai T, Suzuki A, Nakamura Y, Sawamoto K, Ogawa Y, Toyawa Y, Miyata T, Okano H: Musashi1: an evolutionally conserved marker for CNS progenitor cells including neural stem cells. Dev Neurosci 2000, 22:139–153
20. Okano H, Imai T, Okabe M: Musashi: a translational regulator of cell fate. J Cell Sci 2002, 115:1355–1359
21. Sakakibara S, Nakamura Y, Satoh H, Okano H: RNA-binding protein Musashi2: developmentally regulated expression in neural precursor cells and subpopulations of neurons in mammalian CNS. J Neurosci 2001, 21:8091–8107
22. Keyoung HM, Roy NS, Benraiss A, Louissaint Jr A, Suzuki A, Hashimoto M, Rashbaum WK, Okano H, Goldman SA: High-yield selection and extraction of two promoter-defined phenotypes of neural stem cells from the fetal human brain. Nature Biotechnol 2001, 19:843–850
23. Okabe M, Imai T, Kurusu M, Hiromi Y, Okano H: Translational repression determines a neuronal potential in *Drosophila* asymmetric cell division. Nature 2001, 411:94–98
24. Pinus DW, Keyoung HM, Harrison-Restelli C, Goodman RR, Fraser RA, Edgar M, Sakakibara S, Okano H, Nedergaard M, Goldman SA: Fibroblast growth factor-2/brain-derived neurotrophic factor-associated maturation of new neurons generated from adult human subependymal cells. Ann Neurol 1998, 43:576–585
25. Nakamura M, Okano H, Blendy JA, Montell C: Musashi, a neural RNA-binding protein required for Drosophila adult external sensory organ development. Neuron 1994, 13:67–81
26. Sakata S, Kitsukawa T, Kaneko T, Yamamori T, Sakurai Y: Task-dependent and cell-type-specific Fos enhancement in rat sensory cortices during audio-visual discrimination. Eur J Neurosci 2002, 15:735–743
27. Kaneko T, Urade Y, Watanabe Y, Mizuno N: Production, characterization, and immunohistochemical application of monoclonal antibodies to glutaminase purified from rat brain. J Neurosci 1987, 7:302–309
28. Kaneko T, Kang Y, Mizuno N: Glutaminase-positive and glutaminase-negative pyramidal cells in layer VI of the primary motor and somatosensory cortices: a combined analysis by intracellular staining and immunocytochemistry in the rat. J Neurosci 1995, 15:8362–8377
29. Schnell SA, Staines WA, Wessendorf MW: Reduction of lipofuscin-like autofluorescence in fluorescently labeled tissue. J Histochem Cytochem 1999, 47:719–730
30. Martin BM: Cell viability. Tissue Culture Techniques: An Introduction. Boston, Birkhäuser, 1994, pp 61–63

31. Higgins D, Banker G: Primary dissociated cell cultures. Culturing Nerve Cells, ed 2. Edited by G Banker, K Goslin. Cambridge, MIT Press, 1998, pp 37–78
32. Haugland RP: Nucleic acid detection. Handbook of Fluorescent Probes and Research Chemicals, ed 6. Edited by MTZ Spence. Eugene, Molecular Probes, 1996, pp 143–178
33. Haugland RP: Assays for cell viability, proliferation and function. Handbook of Fluorescent Probes and Research Chemicals, ed 6. Edited by MTZ Spence. Eugene, Molecular Probes, 1996, pp 365–398
34. Haugland RP: Nucleic acid detection (Chapter 8) and Assays for cell viability, proliferation and function (Chapter 15). Handbook of Fluorescent Probes and Research Chemicals, ed 7. Eugene, Molecular Probes, 1999
35. Abe K, Saito H: Amyloid β protein inhibits cellular MTT reduction not by suppression of mitochondrial succinate dehydrogenase but by acceleration of MTT formazan exocytosis in cultured rat cortical astrocytes. Neurosci Res 1998, 31:295–305
36. Brustovetsky N, Brustovetsky T, Jemmerson R, Dubinsky JM: Calcium-induced cytochrome c release from CNS mitochondria is associated with the permeability transition and rupture of the outer membrane. J Neurochem 2002, 80:207–218
37. Nogueron MI, Porgilsson B, Schneider WE, Stucky CL, Hillard CJ: Cannabinoid receptor agonists inhibit depolarization-induced calcium influx in cerebellar granular neurons. J Neurochem 2001, 79: 371–381
38. Leslie KR, Nelson SB, Turrigiano GG: Postsynaptic depolarization scales quantal amplitude in cortical pyramidal neurons. J Neurosci 2001, 21:RC170:1–6
39. Brizzee KR, Harkin JC, Ordy JM, Kaack B: Accumulation and distribution of lipofuscin, amyloid, and senile plaques in the aging nervous system. Aging, vol 1. Edited by H Brody, D Harman, JM Ordy. New York, Raven Press, 1975, pp 39–78
40. Lue L-F, Brachova L, Walker DG, Rogers J: Characterization of glial cultures from rapid autopsies of Alzheimer's and control patients. Neurobiol Aging 1996, 17:421–429
41. Rétaux S, Julien JF, Besson MJ, Penit-Soria J: Expression of GAD mRNA in GABA interneurons of the rat medial frontal cortex. Neurosci Lett 1992, 136:67–71
42. Mesulam M-M, Hersh LB, Mash DC, Geula C: Differential cholinergic innervation within functional subdivisions of the human cerebral cortex: a choline acetyltransferase study. J Comp Neurol 1992, 318: 316–328
43. Akiyama H, Kaneko T, Mizuno N, McGeer PL: Distribution of phosphate-activated glutaminase in the human cerebral cortex. J Comp Neurol 1990, 297:239–252
44. Hendry SH, Schwark HD, Jones EG, Yan J: Numbers and proportions of GABA-immunoreactive neurons in different areas of monkey cerebral cortex. J Neurosci 1987, 7:1503–1519
45. Fabri M, Manzoni T: Glutamate decarboxylase immunoreactivity in corticocortical projecting neurons of rat somatic sensory cortex. Neuroscience 1996, 72:435–448
46. Tecoma ES, Choi DW: GABAergic neocortical neurons are resistant to NMDA receptor-mediated injury. Neurology 1989, 39:676–682
47. Grabb MC, Choi DW: Ischemic tolerance in murine cortical cell culture: critical role for NMDA receptors. J Neurosci 1999, 19:1657–1662
48. Mynlieff M: Dissociation of postnatal hippocampal neurons for short term culture. J Neurosci Methods 1997, 73:35–44
49. Kasashima S, Kawashima A, Muroishi Y, Futakuchi H, Nakanishi I, Oda Y: Neurons with choline acetyltransferase immunoreactivity and mRNA are present in the human cerebral cortex. Histochem Cell Biol 1999, 111:197–207
50. Cooper JR, Bloom FE, Roth RH: Amino acid transmitters. The Biochemical Basis of Neuropharmacology, ed 6. New York, Oxford University Press, 1991, pp 133–189
51. Altman FP: Tetrazolium Salts and Formazans. Stuttgart, Gustav Fischer Verlag, 1976, pp 1–56
52. Thibault O, Porter NM, Chen K-C, Blalock EM, Kaminker PG, Clodfelter GV, Brewer LD, Landfield PW: Calcium dysregulation in neuronal aging and Alzheimer's disease: history and new directions. Cell Calcium 1998; 24: 417–433
53. Verkhratsky A, Toescu EC: Calcium and neuronal ageing. Trends Neurosci 1998, 21:2–7